Particle Excursions in Colloidal Crystals

Mischa Megens* and Willem L. Vos

Van der Waals–Zeeman Instituut, Universiteit van Amsterdam,, NL-1018 XE, Amsterdam, The Netherlands[†]
(Received 12 July 2000)

We have performed synchrotron small-angle x-ray diffraction experiments on charge-stabilized colloidal crystals. The mean squared displacements, obtained from Debye-Waller factors, decrease with increasing density beyond freezing. *Irrespective* of the range of the repulsion, our data and previous results lie on a common curve, linearly scaled between the melting and close-packed densities. Surprisingly, the excursions are smaller than predicted by theory.

Understanding how structures in many-body systems arise from their constituents' interactions remains one of the outstanding problems in physics [1–3]. Deeper understanding calls for careful measurements of both the interactions and the resulting structure and dynamics. The interaction between colloidal spheres was studied in-depth by Murray *et al.,* who determined the interaction from the random motion of polystyrene spheres using optical microscopy [1,4]. The observed pair interactions appear to agree reasonably well with the Derjaguin-Landau-Verwey-Overbeek theory of screened electrostatic interaction [4]. However, it is a subject of current debate whether or not the interaction among many spheres is simply a sum of pair interactions [5,6], and the direct visualization of the three-dimensional cooperative motion in dense systems has been reported only recently [7]. Furthermore it is important to understand the role of the suspension liquid, i.e., how the viscous damping and random forces affect the dynamics [8,9]. Brownian motion in systems where many particles interact, such as colloidal crystals, has been observed mostly in two-dimensional layers of colloids near a wall [1,6,10]. The sample walls influence the dynamics considerably: measurements of the single particle dynamics in crystalline layers near a glass wall have revealed a systematic increase of the excursions with increasing distance from the glass plate [10]. We studied bulk three-dimensional colloidal crystals, thus minimizing the effects of the walls of the sample container [8,10,11].

In systems where many particles interact, such as colloidal crystals, the interactions give rise to sound modes, i.e., motions of the particles about their lattice sites. Lindsay and Chaikin [12], and Hurd *et al.* [13] studied the dispersion of sound modes sustained by the combined system of particles and suspension liquid in colloidal crystals, and recently Riese and Wegdam demonstrated the importance of viscous coupling between particles [14]. The excursions of particles from their lattice sites are directly related to the lattice dynamics. The excursions are important in relation to the melting transition: according to the Lindemann criterion, crystals melt at a specific ratio of the extent of the excursions to the interparticle spacing [15,16].

We have systematically mapped out the extent of the excursions as a function of density, by recording small-angle x-ray diffraction patterns of dense colloids as the melting transition is approached. In contrast, previous studies focused mostly on dilute samples at a fixed density ~5 vol% [10,17]. We have rescaled the density in such a way that it interpolates linearly between the density of melting and the close packed density of 74 vol%. As a result, the particle excursions scale onto a common curve, regardless of the type of interaction. Surprisingly, the measured excursions are generally smaller than predicted by theory. Small particle excursions are favorable for the use of colloids as photonic crystals.

We analyzed x-ray diffraction patterns from two samples made of sedimented 100.8 nm radius monodisperse polystyrene spheres (Duke Scientific PS5020A) in methanol. The suspensions were deionized with ion exchange resin (BioRad AG501-X8) before being introduced in thin-walled glass capillaries. Extra ion exchange resin was added to one of the samples. Both samples were centrifuged at $400g$, corresponding to low Peclet numbers of about 0.02, for 3.3 h and then left to equilibrate for two months. The density in the capillaries decreases with height from ~39 to ~52 vol%. We have determined the height of the crystal-liquid interface by visual inspection of the bright green optical Bragg reflection. The density profile is obtained from the x-ray diffraction patterns. Even the dense parts of the samples crystallized and did not form a glass, as evidenced by the large number of fcc peaks. The diffraction patterns were measured at beamline 4 of the European Synchrotron Radiation Facility in Grenoble [18–20].

Two diffraction patterns from the sample with no extra resin are shown in Fig. 1a, one from a dilute suspension with a particle density of <1 vol% and one from a polycrystalline sample region with a density of 45 vol%. The diffracted intensities vs scattering vector $s = 2\sin(\theta)/\lambda$ were obtained at an x-ray wavelength λ of 0.14725 nm. Both diffraction patterns show many interference fringes. The spacing of the fringes reveals the size of the colloidal spheres (radius 100.8 nm). The presence of a large number of fringes indicates that the spheres all have the same size
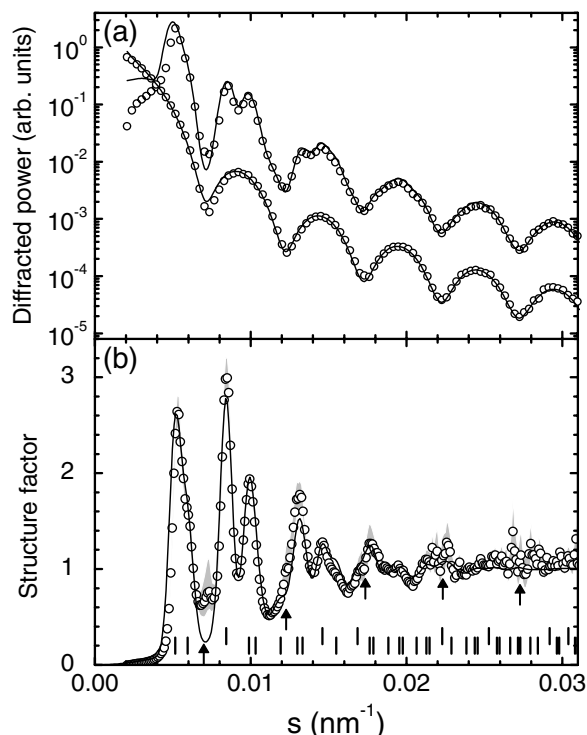
FIG. 1. (a) X-ray diffraction patterns from 100.8 nm radius polystyrene colloidal spheres in methanol, at low density (<1 vol%, lower curve, form factor) and crystallized (45 vol%, no added resin, upper curve). (b) Structure factor (∘), obtained from the data in (a), together with a model curve for fcc crystals with displacements $u = 19.4 \pm 0.5$ nm, lattice parameter $a = 335.5 \pm 0.7$ nm, and 8.7 ± 1.0% preferred orientation [26] (—, both panels). The shaded area indicates the experimental accuracy, estimated from Poisson counting statistics and the agreement between measured and calculated data, that was used in the fit. The arrows indicate the minima in the form factor, where the structure factor is less reliable. The marks for reflections from crystals aligned to the cell walls are shifted up.

(polydispersity 2.1%). Because the colloidal spheres are so monodisperse, they readily form crystals at high densities. The effect of particle shape and spatial arrangement can be separated by dividing the diffraction pattern of the crystal by that of the dilute suspension. Thanks to the high brilliance of the x-ray source, we enjoy the luxury of dividing by a measured form factor, hence the structure factors are completely experimentally determined.

The structure factor, Fig. 1b, consists of the Bragg peaks associated with the crystal lattice. The peak heights reveal the extent of the excursions of the particles from their lattice sites. The excursions reduce the height of the Bragg peak at scattering vector s by the Debye-Waller [21] factor $\exp(-2M)$, with $M = (2\pi su)^2/6$, assuming that the spatial distribution is a Gaussian with rms width u, which is appropriate even for hard spheres [22]. The intensity that disappears from the Bragg peaks reemerges as a diffuse background $1 - \exp(-2M)$ if the motions of the particles are uncorrelated. Correlated particle motions, i.e., sound waves, give structure to the diffuse background, known as thermal diffuse scattering (TDS)

[23,24]. Thermal diffuse scattering tends to accumulate near the Bragg peaks, the peaks acquire "feet" of diffuse intensity. In our case the Bragg peaks and the diffuse peaks are indistinguishable due to limited instrumental resolution. The rms displacement u slightly underestimates the true displacements since the peak areas P_{hkl} include a contribution P_{TDS} due to phonons. Assuming a linear dispersion relation for the phonons, Warren finds that for fcc crystals $P_{TDS}/P_{hkl} \approx Ma\Delta s$, where a is the cubic lattice parameter and $\Delta s \sim 1~\mu m^{-1}$ is the total width of the measured peak [23]. We infer that our rms displacements u underestimate the true rms displacements by only $a\Delta s/4 \sim 8$%. Thus, u can be determined with great accuracy from the diffraction patterns.

The other important ingredient in the peak heights is the multiplicity of the reflections, i.e., the number of reflections with the same scattering vector. The crowding of reflections at large s, apparent from the ticks in Fig. 1b, is compensated by two geometrical factors: at large s, relatively few lattice vectors are close to the Ewald plane; and the size of the ring on the detector is larger [23]. As a result, the peaks in the calculated structure factor coalesce to form a uniform background at large s, and the peak-to-background ratio is fixed right from the start. We fitted the model described above to the experimentally determined structure factors, taking into account the instrumental broadening and the extra intensity in reflections from crystallites with a preferred orientation aligned with the cell walls [18,19]. The resulting model curve is shown in Fig. 1b. The match with the experimental data is striking; it confirms that the crystal structure is indeed fcc [18,19]. From our single crystal diffraction study [19,25] we can put conservative upper bounds on the amount of hcp or randomly stacked planes of 5 and 10 vol%, respectively. The small feature at 0.007 nm^{-1} is an artifact caused by the minimum in the form factor. For the structure factor in Fig. 1b we find a ratio of intensities $I_{\parallel}/I_r$ from aligned vs randomly oriented crystallites of 2.7 ± 0.3, which corresponds to a $\sim(8.7 \pm 1.0)$% fraction of aligned crystallites [26]. The aligned fraction in various samples does not vary in any systematic way with the excursions u, and is generally below 10%. The peaks from the aligned crystallites are relatively strong because the patterns were recorded with the x-ray beam perpendicular to the crystal face, so the Bragg condition is satisfied for all the aligned planes simultaneously. The fitted width of the peaks, $\sigma = 3.8 \times 10^{-4}$ nm^{-1}, agrees well with the measured width of the attenuated direct beam on the detector, $\sigma = 4.0 \times 10^{-4}$ nm^{-1}. From the decrease in peak height with increasing scattering vector we find a rms displacement u of 19.4 ± 0.5 nm.

We determined excursions and lattice spacings at various heights in our colloidal samples. From the lattice spacings and the sphere radius we have deduced the density profile. The results are shown in Fig. 2. The extent of the excursions increases almost in proportion to the lattice spacing. The rms displacements from the two samples form a
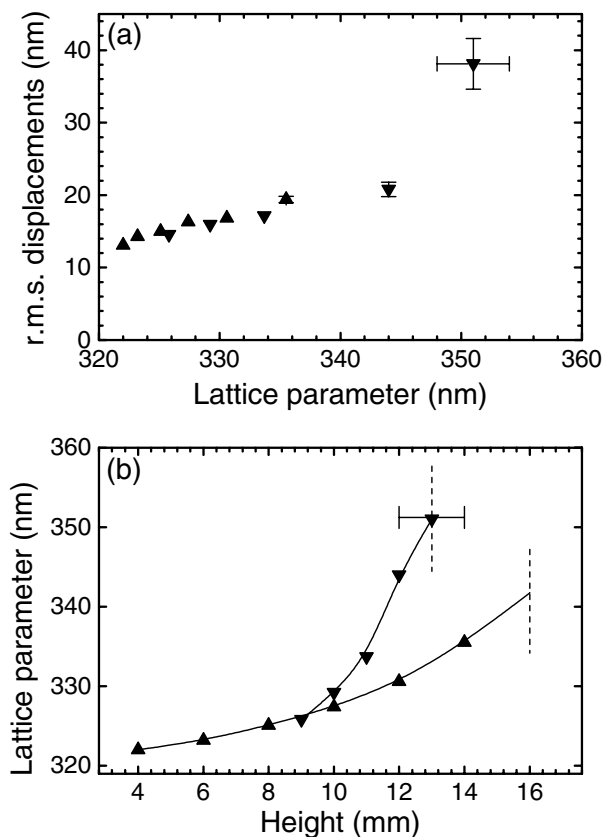
FIG. 2. (a) rms displacements u of the spheres from their equilibrium position, as a function of the cubic lattice parameter, at various heights in two samples of polystyrene spheres in methanol, with (▼) or without (▲) added resin. (b) The density profiles of these samples. The curves are guides to the eye. The top of the crystalline part of the samples is indicated by dashed lines.

FIG. 3. rms displacements u of the spheres from their equilibrium position divided by the nearest neighbor distance d_{nn}, as a function of scaled density, obtained from the data in Fig. 2 (▼, ▲), and from Refs. [17] (▽), [28] (□), and [29] (◇). The dashed line is a numerical result for hard spheres [22].

single curve, although the density profiles in the samples differ considerably: the colloid in the sample with added resin is more compressible, and it has a lower melting density. According to the pressure equation [27], an increased compressibility is indicative of a softer potential, i.e., a more extended double layer. Indeed the more compressible sample is the one which contains extra ion exchange resin. The reduced melting density also indicates that this sample has a more extended double layer. The presence of an extended double layer would imply that there is less room for excursions at the same density, but the rms displacements are very similar despite the difference in screening length. Nevertheless, such similarity is consistent with the condition that has become widely known as the Lindemann criterion of melting [15].

In the spirit of the Lindemann criterion we have plotted in Fig. 3 the ratio $L = u/d_{nn}$ of the displacements u to the nearest neighbor distances d_{nn}. As expected, the normalized displacements L increase as we approach the density of melting. We have rescaled the density axis of the plot in such a way that it ranges from the density of melting to the close-packed density. This rescaling allows us to compare colloidal systems with very different inter-
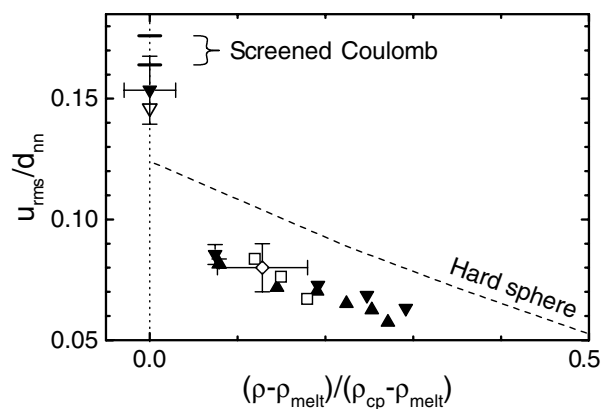
actions, from strongly charged dilute to dense hard-sphere-like systems; the increased range of repulsion of charged spheres is taken into account as a larger "effective" radius. With this new scaling, the normalized displacements from the two samples form a single curve, although the ionic strengths of the samples differ. The dynamic light scattering results of Piazza and Degiorgio [28] on index matched, charged samples with a much lower melting density of 7 vol % are in good agreement with our results. Interestingly, data on sterically stabilized colloids by Cheng et al. [29] agree very well with the scaling proposed here. Apparently, when plotted in this fashion, the relation between the excursions and the particle density is insensitive to the range and type of interparticle interaction.

For hard spheres, calculated normalized displacements are available for a range of densities above the melting transition [22]. We have included these in Fig. 3 for comparison. The measured excursions are clearly smaller than the theoretical hard-sphere results, even if we take into account thermal diffuse scattering. Correcting for the size polydispersity of our spheres would even increase the discrepancy. Because of the good agreement between the experimental results on different colloidal systems, it seems unlikely that the type of repulsive interaction (i.e., long-ranged charged or short-ranged steric) can remedy the discrepancy.

Our Lindemann ratio at the density of melting of 0.150 ± 0.015 is clearly higher than the normalized displacements well into the solid phase. Bierbaum et al. [17] obtained a ratio $L = 0.146$ in a very dilute (0.19 vol %) strongly charged bcc crystal, in very good agreement with our data. These data are slightly smaller than numerical predictions for spheres with a screened Coulomb interaction [8,30]. Numerical simulations for fcc crystals with various ionic strengths, properly extrapolated to infinite system size, predict Lindemann ratios in the range $0.164-0.176$ [30]. The experimental and theoretical Lindemann ratios for charged spheres are clearly higher than the computer simulation result for hard spheres [22].

Remarkably, however, the observed excursions at higher densities are consistently lower than the hard-sphere normalized displacements.

We conclude that small-angle x-ray diffraction makes it possible to study systematically the approach to melting of colloidal crystals. This valuable scattering technique complements recently developed methods based on direct imaging of the particles with microscopy using visible light [1,6,10]. X-ray diffraction provides ample freedom to choose an experimental system since it is not hampered by multiple scattering and therefore refractive index matching is not required. In particular, the technique would be very suitable to study high density systems with attractive interactions. Diffraction offers excellent statistics: the results are based on very large numbers of particles, $\sim 10^8$. The majority of these particles are far away from the sample cell wall, i.e., in the bulk of the crystal. Thus surface effects are eliminated. We find that the excursions in crystals of both charge-stabilized and steric colloidal spheres are generally smaller than the predicted hard-sphere results. The difference may be caused by many-body interactions [6], or by the role of the suspending liquid [8,9]. It would be fruitful to perform lattice dynamics calculations for screened Coulomb pair interactions at various screenings and densities to compare with the results presented here.

High resolution measurements on colloidal single crystals open up the prospect of studying the thermal diffuse scattering, revealing the structure of sound modes in these crystals. Recently, x-ray diffraction was also extended to dynamic measurements, analogous to dynamic light scattering, by exploiting the interference of coherent x rays [31]. With this dynamic technique it will be possible to determine not only the extent of the excursions but also the associated frequencies.

---

*Present address: Department of Physics, Princeton University, Princeton, New Jersey 08544.
†www.complexfluids.com

[1] C. A. Murray and D. G. Grier, Annu. Rev. Phys. Chem. **47**, 421 (1996).

[2] P. M. Chaikin and T. C. Lubensky, *Principles of Condensed Matter Physics* (Cambridge University Press, Cambridge, UK, 1995).

[3] W. Poon, P. Pusey, and H. Lekkerkerker, Phys. World **9**, 27 (1996).

[4] J. C. Crocker and D. G. Grier, Phys. Rev. Lett. **73**, 352 (1994); *ibid.* **77**, 1897 (1996).

[5] A. E. Larsen and D. G. Grier, Nature (London) **385**, 230 (1997).

[6] J. A. Weiss, A. E. Larsen, and D. G. Grier, J. Chem. Phys. **109**, 8659 (1998).

[7] W. K. Kegel and A. van Blaaderen, Science **287**, 290 (2000); E. R. Weeks, J. C. Crocker, A. C. Levitt, A. Schofield, and D. A. Weitz, Science **287**, 627 (2000).

[8] M. O. Robbins, K. Kremer, and G. S. Grest, J. Chem. Phys. **88**, 3286 (1988).

[9] E. R. Dufresne, T. M. Squires, M. P. Brenner, and D. G. Grier, Phys. Rev. Lett. **85**, 3317 (2000).

[10] J. Bongers and H. Versmold, J. Chem. Phys. **104**, 1519 (1996); J. Bongers, H. Manteufel, K. Vondermassen, and H. Versmold, Colloids Surf. A **142**, 381 (1998).

[11] S. Tandom, R. Kesavamoorthy, and S. A. Asher, J. Chem. Phys. **109**, 6490 (1998).

[12] H. M. Lindsay and P. M. Chaikin, J. Chem. Phys. **76**, 3774 (1982).

[13] A. J. Hurd, N. A. Clark, R. C. Mockler, and W. J. O'Sullivan, Phys. Rev. A **26**, 2869 (1982).

[14] D. O. Riese and G. H. Wegdam, Phys. Rev. Lett. **82**, 1676 (1999).

[15] F. A. Lindemann, Phys. Z. **11**, 609 (1910).

[16] *Rare Gas Solids* edited by M. L. Klein and J. A. Venables (Academic, London, 1977).

[17] A. Bierbaum, C. H. Dux, and H. Versmold, Mol. Phys. **93**, 615 (1998).

[18] M. Megens, C. M. van Kats, P. Bösecke, and W. L. Vos, J. Appl. Crystallogr. **30**, 637 (1997).

[19] W. L. Vos, M. Megens, C. M. van Kats, and P. Bösecke, Langmuir **13**, 6004 (1997); Langmuir **13**, 6120 (1997).

[20] P. Bösecke, O. Diat, and B. Rasmussen, Rev. Sci. Instrum. **66**, 1636 (1995).

[21] P. Debye, Ann. Phys. (Leipzig) **43**, 49 (1914); I. Waller, Z. Phys. **17**, 398 (1923).

[22] D. A. Young and B. J. Alder, J. Chem. Phys. **60**, 1254 (1974); A. Kyrlidis and R. A. Brown, Phys. Rev. E **47**, 427 (1993).

[23] B. E. Warren, *X-ray Diffraction* (Addison-Wesley, Reading, MA, 1975).

[24] P. A. Rundquist, R. Kesavamoorthy, S. Jagannathan, and A. Asher, J. Chem. Phys. **95**, 1249 (1991).

[25] M. Megens, Ph.D. thesis, Universiteit van Amsterdam, 1999, available from our website.

[26] The accuracies quoted for the fraction of aligned crystallites $f = (I_\parallel/I_r)/(c^*\ell)$ are based on the accuracies of $I_\parallel/I_r$ and the reciprocal lattice vector $c^* = \sqrt{3}/a$, leaving aside a possible systematic error in the transverse coherence length $\ell \sim 6 \; \mu$m [25].

[27] J. P. Hansen and I. R. McDonald, *Theory of Simple Liquids* (Academic, London, 1986).

[28] R. Piazza and V. Degiorgio, Phys. Rev. Lett. **67**, 3868 (1991).

[29] Z. Cheng, J.-X. Zhu, W. B. Russel, and P. M. Chaikin, Phys. Rev. Lett. **85**, 1460 (2000). The density of the crystals is 57 ± 1 vol % [Z. Cheng, (private communication)].

[30] E. J. Meijer and D. Frenkel, J. Chem. Phys. **94**, 2269 (1991); M. J. Stevens and M. O. Robbins, J. Chem. Phys. **98**, 2319 (1993).

[31] D. O. Riese, W. L. Vos, G. H. Wegdam, F. J. Poelwijk, D. L. Abernathy, and G. Grübel, Phys. Rev. E **61**, 1676 (2000), and references therein.